Thermochimica Acta, 27 (1978) 285–297

STUDY OF URANYL FORMATE THERMOLYSIS

MICHÈLE BIDEAU AND BERNARD CLAUDEL*

Laboratoire de Cinétique et Génie Chimiques, 404-INSA, 20 avenue Albert Einstein, F-69621 Villeurbanne (France)

(Received 23 January 1978)

ABSTRACT

In order to evidence the different intermediate steps of the thermolysis of uranyl formate, a study has been made of the different parameters which influence this decomposition. The use of mass spectrometry and of gas chromatography allowed us to identify CO, CO_2, H_2O and HCOOH as evolved gases and to measure their respective amounts. The "primary" products are CO and HCOOH. It is shown that these two species react in the presence of the solid α-UO_3 formed by the primary reaction. Carbon monoxide reduces the solid to the lower oxides U_3O_8, U_2O_9 and finally UO_2. HCOOH is selectively decomposed by the catalytic action of the solid to CO and H_2O. These results allow us to put forward a mechanism of decomposition in which, after the decarboxylation

$$UO_2(HCOO)_2 \rightarrow \alpha\text{-}UO_3 + HCOOH + CO$$

the two reactions

$$HCOOH \rightarrow CO + H_2O$$

$$UO_3 + x\,CO \rightarrow x\,CO_2 + UO_{3-x}$$

take place, the kinetics of which have been measured and shown to be in agreement with that of the overall reaction.

INTRODUCTION

Carboxylates, and especially formates, have long been studied with respect to their thermal stability and the nature of gases evolved during their thermal decomposition. However, relatively few researches have been devoted to determining, among the reactions occurring during this thermolysis, which are the primary and which the secondary ones, although the importance of this distinction has been pointed out in this laboratory in the case of thorium formate[1]. As a matter of fact, the primary

* To whom all correspondence concerning this article should be addressed.

products are generated in the presence of a finely divided solid, and may yield a great variety of secondary products, as amply demonstrated by the diversity of the results reported for the formates[2-8].

More specifically, uranyl formate has been decomposed by Lyden[9] in a CO_2 atmosphere. The products obtained are CO, CO_2, H_2O and a black oxide, U_3O_8, which is considered as a primary product. Buttress and Hughes[10] followed the decomposition by thermogravimetric analysis in air and in argon and found that the green solid formed between 245°C and 340°C consisted mainly of α-UO_3 and a small amount of UO(OH)(HCOO) which decomposed only above 370°C. The kinetics of the decarboxylation of uranyl formate obeys Prout–Tompkins law with an activation energy of 40.4 (± 1) kcal mole^{-1}. At 280°C, under reduced pressure, these authors obtained CO, CO_2, H_2, H_2O and HCOOH, so that they wrote the overall balance

$$3\ UO_2(HCOO)_2 \rightarrow 3\ \alpha\text{-}UO_3 + 2\ HCOOH + 4\ CO + H_2O$$

The detected hydrogen would come from a slight dehydrogenation of formic acid. The evolution of CO_2 is claimed to be due to the formation of UO(OH)(HCOO) as a by-product.

More recently, Russell and Hyder[11] observed, during the decomposition of $UO_2(HCOO)_2 \cdot H_2O$, a break in the thermogravimetric curve at 200°C. This break was ascribed to $UO_2(OH)(HCOO)$, but without any identification of this compound. The second break observed in the curve was at 285°C and corresponded to $UO_3 \cdot 0.8\ H_2O$, the evolved gases being mainly CO with traces of H_2O. When $UO_2(HCOO)_2$ was decomposed below 300°C under the pressure of the evolved gases only, CO_2 was found in the gas phase, and the solid was claimed to be $UO_2 \cdot H_2O$.

EXPERIMENTAL

Starting material

Uranyl formate monohydrate was prepared according to the procedure by Sahoo et al.[12], i.e. by reacting formic acid with uranyl nitrate. The anhydrous salt was obtained by heating the monohydrate at 150°C under continuous pumping at 10^{-3} torr for 1 h. For the sake of reproducibility, we restricted our investigation to samples of the starting material the grain diameter of which was between 125 and 160 μm.

Gas phase analysis

The reaction cell was included in a loop allowing the recycling of the gases with the help of a circulation pump[13]. Their total pressure was determined manometrically and their composition by gas chromatography. The carrier gas was helium and the column was packed with Porapak Q, 80–100 mesh. The amount of a gaseous component is expressed as the number of moles, n, per mole of the anhydrous salt $UO_2(HCOO)_2$. The results concerning formic acid, which in the gas phase is partially dimerized[14, 15], are expressed for the sake of clarity in "monomeric equivalents".

Solid phase analysis

Thermogravimetric (TG) analysis was performed with a 4102 type Sartorius balance. Programs of temperature rise and regulation were controlled by a Pyrectron type Coreci apparatus.

Differential thermal analysis (DTA) was carried out with a BDL M3 apparatus on 10 mg samples at a heating rate of 5°C min^{-1} in a nitrogen atmosphere.

The total uranium content of the solid obtained from the decomposition of $UO_2(HCOO)_2$ was obtained by calcination to U_3O_8 (ref. 16) and the U(IV) content by spectrophotometry[17]. For the latter analysis, the solid was dissolved in a warm 10% H_3PO_4 solution under a nitrogen atmosphere, in order to maintain the degree of oxidation of uranium. For the oxide U_3O_8, which contains two U(V) ions for one U(VI) ion[18, 19], the quinquivalent uranium disproportionates into U(VI) and U(IV), the reaction rate increasing with the solution acidity[20]. If the global composition of the obtained uranium oxides is expressed by UO_{3-x}, x is the ratio of the weight percentage of uranium(IV) to the weight percentage of total uranium.

Classical organic analysis gave the amounts of the other elements. X-Ray diffraction patterns were obtained with a Kristalloflex II Siemens diffractometer provided with a copper anticathode and a nickel filter. Infrared absorption spectra were obtained in the range 625–4000 cm^{-1} with a 257 type Perkin-Elmer spectrophotometer.

RESULTS

Main features of the decomposition of $UO_2(HCOO)_2$

TG curves have been obtained at a heating rate of 5°C min^{-1} under continuous pumping (pressure of about 10^{-5} torr) and also under the residual pressure of the evolved gases not condensed in a liquid nitrogen trap. In both cases, dehydration is achieved at 180°C, decarboxylation beginning at 280°C and continning up to about 250°C. At this temperature, the two TG curves diverge: that obtained in vacuum becomes horizontal and is located above the continuously decreasing curve obtained under the residual pressure of gases. This latter curve tends to a plateau at much higher temperatures.

The solids obtained at 450°C are different: that from the vacuum decomposition is dark green and its X-ray diffraction pattern reveals the presence of U_3O_8 and α-UO_3 while that formed under the residual pressure of evolved gases is black and its X-ray diffraction pattern corresponds to UO_2.

These results show that the decarboxylation of $UO_2(HCOO)_2$ yields reducing gases which more or less reduce the remaining solid, depending on their contact time with it.

The DTA curve exhibits two well-separated endotherms. Previous approximate standardising of the DTA set-up allowed us to estimate roughly from their respective areas, the enthalpy variation for dehydration, $\Delta H_1 = 15\ (\pm 3)$ kcal $mole^{-1}$, and the enthalpy variation for decarboxylation, $\Delta H_2 = 40\ (\pm 8)$ kcal $mole^{-1}$. These figures

compare well with those recently obtained by Bousquet et al. with a home-built calorimeter[21]. These authors found, for the standard variations of enthalpy of formation, $\Delta H^{\circ}_{hyd.} = -520.6\ (\pm 0.1)$ kcal mole^{-1} for the hydrate, and $\Delta H^{\circ}_{anhyd.} = -447.1\ (\pm 0.1)$ kcal mole^{-1} for the anhydrous salt. Hence, using -57.8 kcal mole^{-1} for the standard heat of formation of water[22], the value $\Delta H_1 = 15.7$ kcal mole^{-1} may be calculated, in agreement with our result. Likewise, using -292 kcal mole^{-1} and -26.4 kcal mole^{-1} for the standard heats of formation of α-UO_3 and CO respectively[22], the value $\Delta H_2 = 38.2$ kcal mole^{-1} may be calculated, again in agreement with our rough estimation.

Study of the gas phase

The pressure increase, ΔP, due to the evolution of gases is represented as a function of time at different temperatures by a monotonically ascending curve which reaches a plateau (obtained after about 20 h at 242°C). In the following, we fixed at 24 h the duration of an isothermal experiment and analysed the composition of the gas obtained after this length of time. Under these conditions, whatever the thermolysis temperature may be, the only gaseous products are CO, CO_2 and H_2O. When the temperature increases, n_{CO} decreases continuously and reaches the plateau $n_{CO} = 1$ (Fig. 1). The same trend is observed for CO_2. Thus, when one mole of formate has been decomposed, two moles of the mixture CO + CO_2 have been formed. On the other hand, n_{H_2O} varies very little in the temperature range 240–300°C and does not reach the expected value ($n_{H_2O} = 1$). This can be explained by the retention by the oxide of part of the water formed, an already reported phenomenon[23], that we can check by submitting the solid to a second heating at 400°C for 12 h and observing that 80–90% of the expected amount of water desorbs. As we shall see below, chemical analysis of the solid residues also confirm this point.

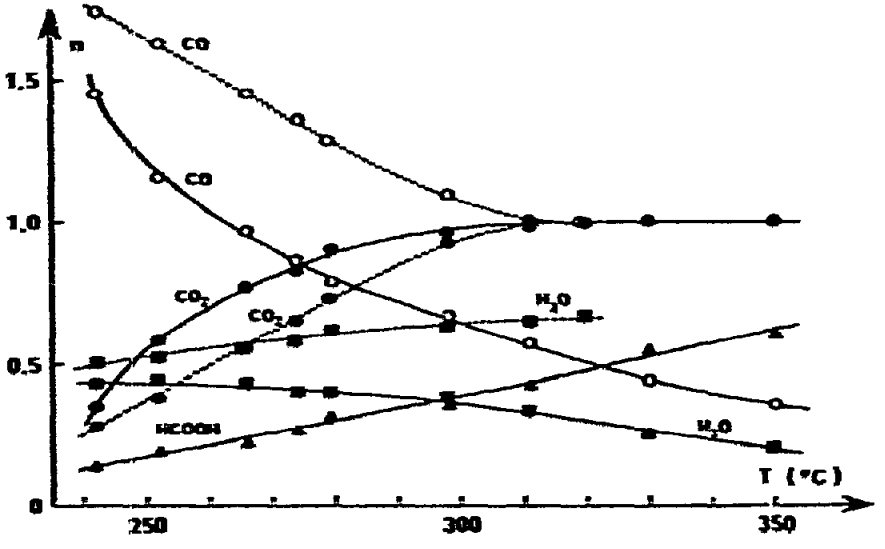

Fig. 1. Influence of decomposition temperature on the gas phase composition. — — — —, Without trap; ———, in the presence of a liquid nitrogen trap.

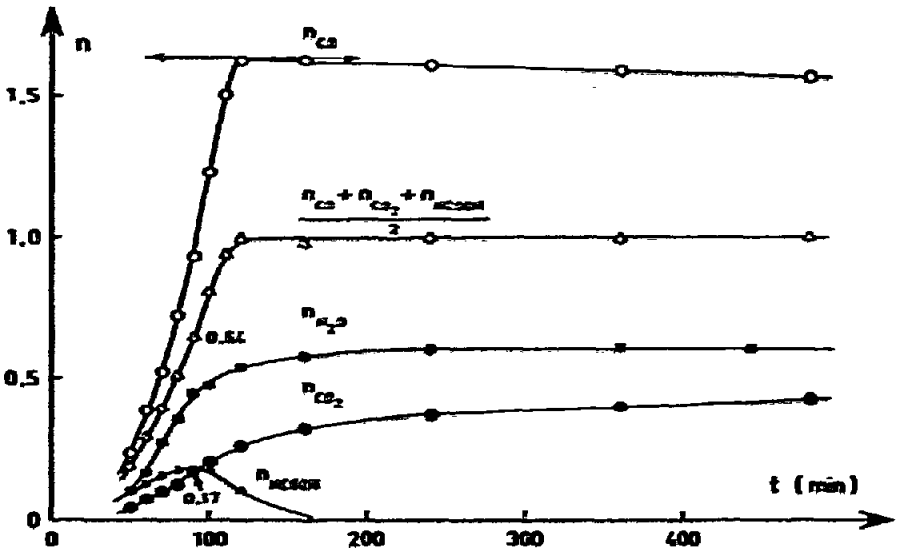

Fig. 2. Gas phase composition as a function of time at 279 °C.

It is also possible, at a given temperature, to follow the composition of the gas phase left in contact with the solid obtained from the decomposition, as a function of the duration of this contact. Figure 2 represents the obtained results. It can be seen that, at the beginning of the decomposition, the rate of CO appearance is very great in comparison with that of the other components. At a time of about 100 min, n_{CO} passes through a maximum and later decreases. HCOOH forms only at earlier times, and vanishes completely at 180 min, which corresponds to a plateau for n_{H_2O} and to a slow increase of n_{CO_2}. The rate of this increase is roughly equal to the rate of decrease of n_{CO}. This means that there is simultaneous production of CO_2 and consumption of CO when the contact between the gases and the solid is prolonged.

In a third series of experiments, the duration was fixed at 24 h, but the evolved gases were contacted with a liquid nitrogen trap. Chromatographic analysis of the non-condensed gas shows that it consists only of carbon monoxide. Again, n_{CO} passes through a maximum. When the decomposition temperature increases, the rates of CO appearance and of CO disappearance increase and the maximum is depressed.

We checked the presence of HCOOH in the condensed gases. Its amount increases with the decomposition temperature, whereas that of H_2O decreases. Comparison of these results with those obtained without the liquid nitrogen trap (Fig. 1) shows that n_{CO_2} increases more rapidly, but tends towards the same limit ($n_{CO_2} = 1$) and n_{CO} decreases more rapidly, crosses the value 1, and seems to tend towards zero for higher decomposition temperatures.

To sum up, the elimination of condensable gases influences the amounts of all the components H_2O, CO, CO_2, HCOOH. The presence of HCOOH may be correlated with an appreciable decrease of the CO and H_2O contents, but does not seem to affect the CO_2 content. As a matter of fact, above 300 °C, n_{CO_2} remains practically constant, whereas a temperature rise causes an increase of n_{HCOOH} and a decrease of n_{CO} and n_{H_2O}.

The nature of the primary gases may be detected by mass spectrometry, by carrying out the decomposition at a lower temperature (220 °C) in order to restrict the interference of secondary reactions. At the beginning of decomposition, the peaks characteristic of CO and HCOOH appear and later decrease simultaneously with the manifestation of the peaks of H_2O and CO_2. This confirms that the first two gases are primary products, and the last two secondary products.

Study of the solid phases

We have measured x by chemical analysis and compared the results with n_{CO_2} previously found. As shown in Table 1 for the lower decomposition temperatures T, the agreement is excellent. The discrepancies grow when the oxide reaches a composition closer to UO_2. This is due to the fact that the very finely divided oxide reoxidises immediately it is brought into contact with air[23].

A very good agreement between x and n_{CO_2} is also found when the latter gas is condensed in a liquid nitrogen trap during the thermolysis.

It is worthy of note that part of the evolved water remains adsorbed by the solid. As a matter of fact, calcination into U_3O_8 allows us to determine the ratio O/U for the oxide. This ratio is always greater than the expected value of $(3 - x)$. This discrepancy is ascribable to water remaining on the solid. If we call its value Δn and add it to n_{H_2O} as previously determined, we obtain a result close to 1 at any decomposition temperature T as indicated by Table 2.

TABLE 1

CHEMICAL AND X-RAY ANALYSES OF THE SOLID RESIDUES

T	n_{CO_2}	x	*Overall composition*	*Phases detected by X-ray diffraction*	*Colour of solid residue*
242	0.28	0.28	$UO_{2.72}$	U_3O_8, α-UO_3	Green
252	0.38	0.38	$UO_{2.62}$	U_3O_8, α-UO_3, U_4O_9	Dark green
266	0.54	0.55	$UO_{2.45}$	U_3O_8, U_4O_9–UO_2 + α-UO_3	Grey
274	0.65	0.64	$UO_{2.36}$	U_4O_9–UO_2 + U_3O_8 + α-UO_3	Dark grey
279	0.73	0.73	$UO_{2.27}$	U_4O_9–UO_2 + U_3O_8	Black
298	0.92	0.88	$UO_{2.12}$	U_4O_9–UO_2	Black
311	0.99	0.91	$UO_{2.09}$	UO_2	Black

TABLE 2

WATER EVOLVED AND REMAINING ON THE SOLID

T	n_{H_2O}	Δn	$n_{H_2O} + \Delta n$
242	0.50	0.48	0.98
252	0.52	0.43	0.95
266	0.56	0.45	1.01
274	0.58	0.41	0.99
279	0.62	0.40	1.02

The X-ray diffraction patterns obtained for each solid residue are generally quite complex. Comparison with literature data allowed us to identify four phases, α-UO_3 (ref. 24), U_3O_8 (ref. 25), U_4O_9 (ref. 26) and UO_2 (ref. 27). In the fifth column of Table 1, the detected phases are reported in the decreasing order of their amounts estimated from the intensity of their diffraction lines. It can be deduced that oxides form in succession α-UO_3, U_3O_8, U_4O_9 and UO_2, this order corresponding to a progressive reduction of the solid. Operating in the presence of a liquid nitrogen trap does not bring any change except that the cubic phase U_4O_9 already appears at 240 °C.

In using krypton as adsorbate, we measured the specific areas of $UO_2(HCOO)_2$, H_2O and of $UO_2(HCOO)_2$, and found 0.09 $m^2\ g^{-1}$ and 0.16 $m^2\ g^{-1}$, respectively. For the oxides, we used nitrogen as adsorbate and found 36 $m^2\ g^{-1}$ for the solid $UO_{2.75}$ obtained under continuous pumping at 350 °C during 24 hours and 43 $m^2\ g^{-1}$ for UO_2. It thus seems that the specific area increases with the reduction of the oxide. This phenomenon has already been observed by Dell and Wheeler[28] and may be attributed to the increase of porosity, which varies proportionally to the density of the solid.

Kinetics of $UO_2(HCOO)_2$ decomposition

Isothermal thermolyses of $UO_2(HCOO)_2$ have been carried out in the presence of the evolved gases. All the TG curves exhibit the same peculiarity, i.e. the absence of a final plateau, owing to the continuous reduction of the solid by gaseous CO. In an

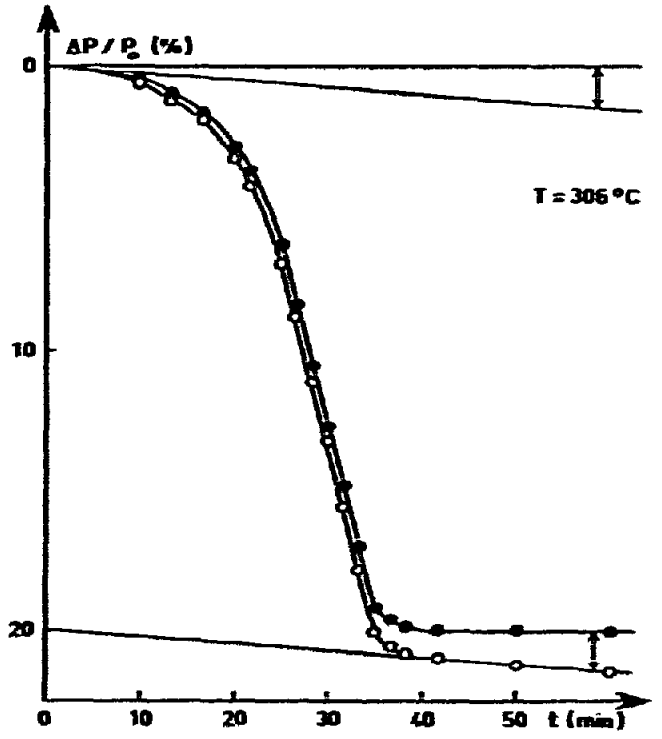

Fig. 3. Example of TG curve correction. —○—○—, Experimental curve; —●—●—, corrected curve.

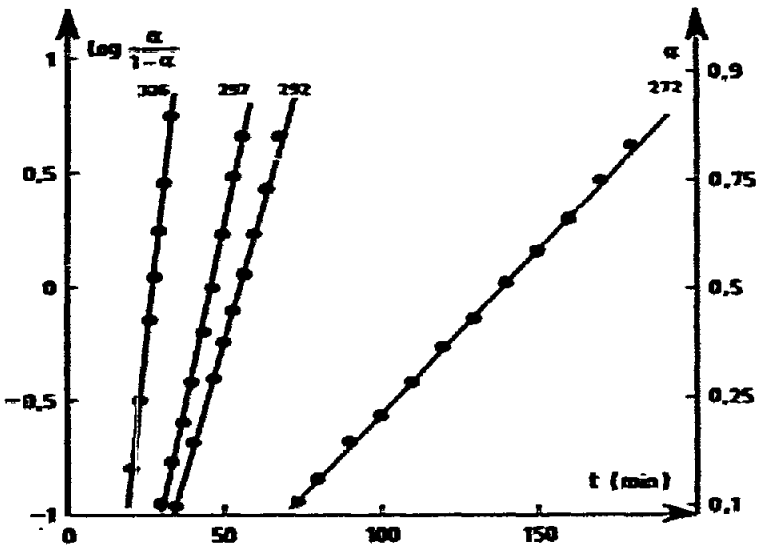

Fig. 4. Linear transforms of experimental curves, according to the Prout and Tompkins law.

attempt to take into account the reduction occurring during decarboxylation, we noticed that the former corresponded, after the completion of the latter, to a linear weight decrease. Therefore we extended this straight line to the region of decarboxylation and obtained the corrected curve by subtracting the straight line from the experimental curve, as indicated by Fig. 3.

It has thus been possible to obtain the values of the fractional decomposition α of $UO_2(HCOO)_2$ into UO_3 at different temperatures. Among the numerous laws which have been put forward, we checked that the best fit was given by that of Prout and Tompkins

$$\log\left(\frac{\alpha}{1-\alpha}\right) = kt + C$$

for $0.10 < \alpha < 0.80$ as shown by Fig. 4. From the straight lines obtained at each temperature, we can deduce k, and, hence, an activation energy equal to 39 ($\pm$ 2) kcal mole^{-1}, in good agreement with the value of 40 ($\pm$ 1) kcal mole^{-1} found by Buttress and Hughes[10].

DECARBOXYLATION MECHANISM

Hypothesis on the reaction steps

In order to account for the previously reported results, we suppose that the primary decarboxylation step is

$$\text{(I)}\quad UO_2(HCOO)_2 \rightarrow \alpha\text{-}UO_3 + HCOOH + CO \qquad (1)$$

the products of which undergo a further evolution according to secondary steps. It is well known[29, 30], that formic acid can decompose according to the three schemes:

$$HCOOH \rightarrow CO + H_2O \quad (2a)$$

$$HCOOH \rightarrow CO_2 + H_2 \quad (2b)$$

$$2\,HCOOH \rightarrow CO_2 + H_2O + HCHO \quad (2c)$$

As we never detected either acetaldehyde or hydrogen, we may retain only the reaction (2a), a dehydration selectively catalysed by the uranium oxides UO_{3-x} formed from α-UO_3. This formation in turn is due to the reduction

$$UO_3 + x\,CO \rightarrow x\,CO_2 + UO_{3-x} \quad (3)$$

which explains the good agreement observed between the amount of evolved CO_2 and the degree of reduction, x.

Under no circumstances did we find the intermediate phases UO(OH)(HCOO) put forward by Buttress and Hughes[10] (its decomposition into α-UO_3 seems unlikely anyhow, at least in a non-oxidizing atmosphere), or UO_2(OH)(HCOO) considered by Russell and Hyder although these solids have been prepared in our laboratory, but in different ways[31-33].

To sum up, reactions (2a) and (3) appear as logical consequences of reaction (1). However, their intervention can only considered as proven if they are directly evidenced and if it is shown that their kinetics agree with that of the overall decomposition[34].

Catalytic dehydration of HCOOH (Fig. 5)

We circulated in a differential flow reactor an helium flux saturated with formic acid vapour by passage through a saturator S, at a fixed temperature, T_S, followed by a condenser C also at a fixed temperature, T_C, lower than T_S. The value of T_C determined the partial pressure of HCOOH as its saturated vapour pressure at T_C. (This pressure was varied between 8 and 60 torr.) The gases flowed out through a trap T cooled by an ice + NaCl mixture, in which water and formic acid condensed, and were directed to a gas chromatograph. A preliminary study allowed us to determine the conditions under which the reaction rate, r_2, (expressed in moles of CO produced per hour and per gram of catalyst) was independent of the flow rate and of the

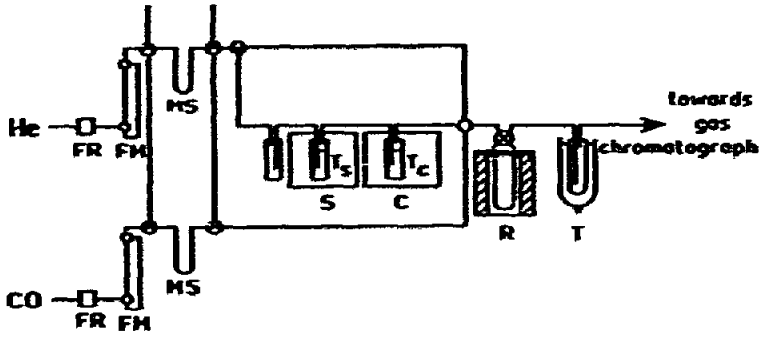

Fig. 5. Set-up for the study of catalytic dehydration of formic acid. FR, Flow regulator; FM, flowmeter; MS, molecular sieve; S, saturator; C, condenser; R, reactor; T, trap.

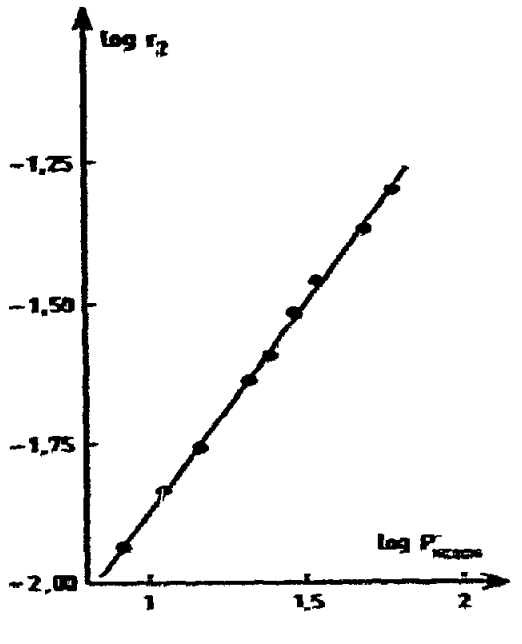

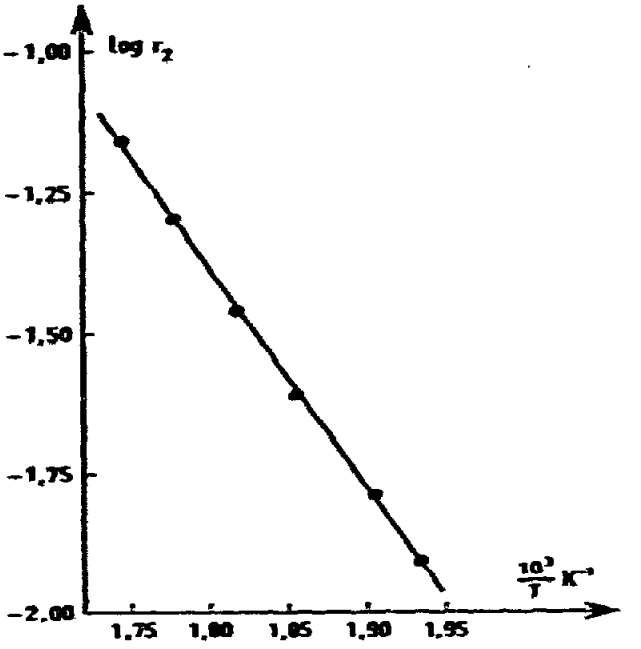

Fig. 6. Apparent order of catalytic dehydration with respect to formic acid at $T = 289$ °C.

Fig. 7. Determination of the activation energy of catalytic dehydration of formic acid.

catalyst mass. The catalyst was α-UO_3 obtained by uranyl formate decomposition in oxygen at 350°C for 24 h. The catalysis temperatures investigated ranged from 240 to 300°C. Under these conditions, CO_2 was observed as a by-product (about 1% of the amount of CO). It has been checked that this CO_2 formation is due solely to a slight, and expected, reduction of the catalyst, that we shall not take into account in the following, owing to its very small extent.

The points representing $\log r_2$ as a function of $\log P_{HCOOH}$ fit a straight line, as indicated by Fig. 6, which refers to a temperature of 289°C. The slope of this straight line, i.e. the apparent order with respect to formic acid, is 0.74 ($\pm$ 0.05). At a fixed partial pressure of HCOOH, the catalyst temperature was varied. A plot of $\log r_2$ as a function of the reciprocal absolute temperature gives a straight line, the slope of which allows us to calculate the apparent activation energy, E_2, equal to 18 ($\pm$ 1) kcal mole^{-1} (Fig. 7).

Reduction for uranium trioxide by carbon monoxide

This reaction has been studied by TG at different temperatures. α-UO_3 was submitted to various partial pressures of carbon monoxide (the volume of the apparatus being large enough to keep constant this pressure during the experiment). The curves giving the extent of reduction, x, of the solid as a function of time exhibit the same feature (Fig. 8, obtained at 280°C). The reduction rate is very fast initially and decreases at about $x = 0.3$. From $x = 0.5$ to 0.8, the rate remains practically constant and then slowly decreases. The same rate decrease at about $x = 0.3$ has been noted

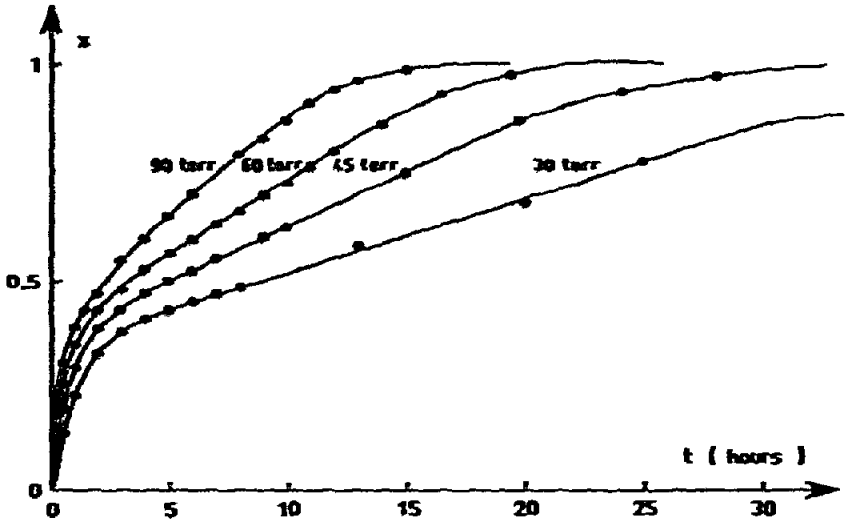

Fig. 8. Reduction of uranium trioxide by CO at T = 280 °C.

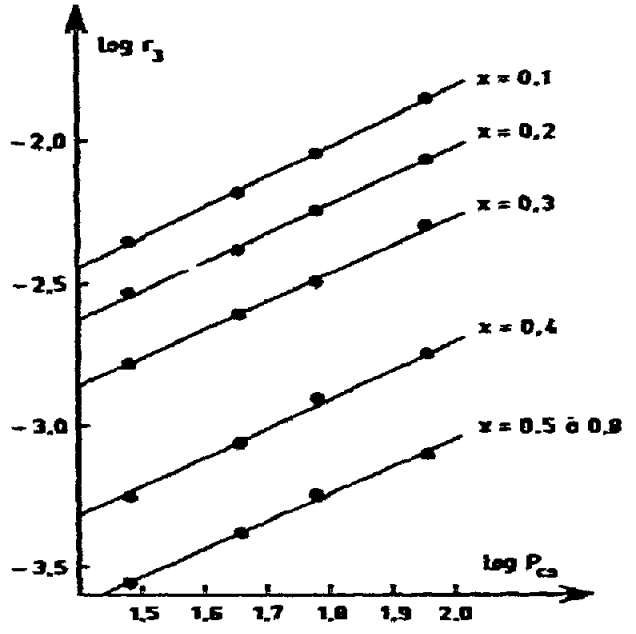

Fig. 9. Variation of log r_3 as a function of log P_{CO} at different reduction extents of uranium trioxide (T = 280 °C).

and ascribed to the formation of U_3O_8 by the different authors[35-37] who have investigated the reduction of uranium oxides, either with hydrogen or with carbon monoxide. At a given reduction, we find, as did Vlasov and Shalaghinov[37], a reaction rate, r_3, proportional to P_{CO} (Fig. 9). At a given partial pressure of CO, the apparent activation energy depends on x.

For $0.1 < x < 0.3$ $\quad E_3 = 20\ (\pm 2)$ kcal mole^{-1}

For $0.5 < x < 0.8$ $\quad E_3 = 34\ (\pm 1)$ kcal mole^{-1}

Comparison of the rates of HCOOH catalytic dehydration and x-UO_3 reduction with the overall decarboxylation rate

Let us call r_i the rate of the ith step. The overall decarboxylation rate (as measured by the number of moles of CO appearing at a definite time, t, per mole of initial salt) is

$$r = r_1 + r_2 - x r_3$$

Let us consider the position of maximum formic acid production $t = 90$ min, $P_{HCOOH} = 6$ torr, according to Fig. 2. At this point, $r_1 = r_2$, $r = 2.8 \times 10^{-2}$ mole of CO min^{-1} and the rate of CO_2 appearance is $x r_3 = 3.5 \times 10^{-3}$ mole of CO_2 min^{-1}. Accordingly, $r_2 \approx 1.6 \times 10^{-2}$ mole of CO min^{-1}. At this point, the extent of decomposition of $UO_2(HCOO)_2$, as given by half the sum of the number of moles of gaseous products containing at least one carbon atom, may be estimated as equal to 0.64. The overall composition of the corresponding solid is $UO_{2.83}$, since $n_{CO_2} = 0.17$.

Let us now compare the value of r_2 so calculated to that found during the catalytic dehydration of HCOOH. At 279 °C, under $P_{HCOOH} = 60$ torr, we find (Fig. 7) 3.7×10^{-2} moles of CO/h g. and hence taking into account the order 0.74 with respect to HCOOH, $r_2' = 6.7 \times 10^{-3}$ moles of CO/h g. In order to convert r_2' into the same units as r_2, we have to keep in mind that r_2 is measured when only 0.64 moles of $UO_2(HCOO)_2$ have been decomposed into an oxide $UO_{2.83}$ of molal weight M. Thus

$$r_2' = \frac{6.7 \times 10^{-3}}{60} \times 0.64 \times M = 2 \times 10^{-2}$$

moles of CO per min and per mole of the initial salt. Thus it can be seen that r_2' is in fair agreement with r_2 if all the approximations made are remembered.

Let us now compare the reduction rate observed during thermolysis with that obtained during the direct reduction of uranium trioxide. For $P_{CO} = 30$ torr and $x = 0.17$, the latter is $x r_3' = 3.2 \times 10^{-3}$ moles of CO_2 per min and per mole of the initial oxide, thus $x r_3' = 2 \times 10^{-3}$ moles of CO per min and per mole of the initial salt, a value which compares well with $x r_3 = 3.5 \times 10^{-3}$.

CONCLUSIONS

Study of the gas and solid phases obtained from $UO_2(HCOO)_2$ thermolysis allowed us to show that three reactions took place. They were (1) the decomposition of the salt into the α variety of uranium trioxide, formic acid and carbon monoxide; (2) the dehydration of formic acid selectively catalysed by the uranium oxides; and (3) reduction of uranium trioxide by carbon monoxide.

It is worth noting that the second step cannot take place on uranium oxides through the intermediate formation of a formate, as suggested by different authors for other oxides[38–40] since it is the reverse reaction of the passage from the formate to formic acid which takes place under these conditions. A 100% selectivity in favour of the dehydration has been observed, which shows the strong acidity of the surface[41].

REFERENCES

1 B. Mentzen, *Ann. Chim.*, 3 (1968) 367.
2 G. Djega-Mariadassou, A. Marques and G. Pannetier, *Bull. Soc. Chim. Fr.*, 9 (1971) 3166.
3 R. Schuffenecker, Y. Trambouze and M. Prettre, *Ann. Chim.*, 7 (1962) 127.
4 T. Meisel, Z. Halmos, K. Seybold and E. Pungor, *J. Therm. Anal.*, 7 (1975) 73.
5 A. K. Galwey and D. M. Jamieson, *J. Phys. Chem.*, 78 (1974) 2662.
6 G. Rama Rao, K. C. Patil and C. N. R. Rao, *Inorg. Chim. Acta*, 4 (1970) 215.
7 D. Dollimore and K. H. Tonge, *J. Inorg. Nucl. Chem.*, 29 (1967) 621.
8 S. Shishido and Y. Masuda, *Nippon Kagaku Kaishi*, 1 (1973) 185.
9 R. Lyden, *Finska Kemistam Finnkets Meddl.*, 74 (1965) 37.
10 G. D. Buttress and M. A. Hughes, *J. Chem. Soc.*, (1968) 1272.
11 E. R. Russell and M. L. Hyder, *Inorg. Nucl. Chem. Lett.*, 12 (1976) 247.
12 B. Sahoo, S. Panda and D. Patnaik, *J. Indian Chem. Soc.*, 37 (1960) 594.
13 J. S. Watson, *Can. J. Technol.*, 34 (1956) 373.
14 A. Coolidge, *J. Am. Chem. Soc.*, 50 (1928) 2166.
15 H. C. Ramsperger and C. W. Porter, *J. Am. Chem. Soc.*, 48 (1926) 1267.
16 B. Grundy and A. Hamer, *J. Inorg. Nucl. Chem.*, 23 (1961) 148.
17 C. J. Rodden, *Analytical Chemistry of the Manhattan Project*, McGraw-Hill, New York, 1950, p. 77.
18 A. F. Andresen, *Acta Crystallogr.*, 11 (1958) 612.
19 R. Sato, *Acta Crystallogr.*, 7 (1961) 763.
20 A. Ekstrom, *Inorg. Chem.*, 13 (1974) 2237.
21 J. Bousquet, B. Bonnetot, P. Claudy, D. Mathurin and G. Turck, *Thermochim. Acta*, 14 (1976) 357.
22 O. Kubachewski and E. L. Evans, *Metallurgical Thermochemistry*, Pergamon Press, New York, 1956.
23 P. Perio, *Rapport CEA No. 363*, 1955.
24 W. Zachariasen, *Acta Crystallogr.*, 1 (1948) 265.
25 F. Gronvold, *Nature (London)*, 162 (1948) 70.
26 B. Belbeoch, C. Pickarski and P. Perio, *Acta Crystallogr.*, 14 (1961) 837.
27 F. Gronvold, *J. Inorg. Nucl. Chem.*, 1 (1955) 357.
28 R. M. Dell and V. J. Wheeler, *Trans. Faraday Soc.*, 58 (1962) 1590.
29 P. Sabatier and A. Mailhe, *C.R. Acad. Sci.*, 152 (1911) 1212.
30 H. Adkins and H. Nissen, *J. Am. Chem. Soc.*, 45 (1923) 809.
31 A. Navarro, *Ann. Chim.*, 6 (1971) 349.
32 B. Claudel, M. Feve, J. P. Puaux and H. Sautereau, *J. Photochem.*, 7 (1977) 113.
33 M. Bideau, R. Bressat, B. Mentzen and A. Navarro, *C.R. Acad. Sci.*, 271 (1970) 225.
34 M. Prettre and B. Claudel, *Elements of Chemical Kinetics*, Gordon and Breach, New York, 1970, p. 71.
35 K. J. Notz and M. G. Mendel, *J. Inorg. Nucl. Chem.*, 14 (1960) 55.
36 E. de Marco and M. G. Mendel, *J. Phys. Chem.*, 64 (1960) 132.
37 V. G. Vlasov and V. N. Shalaghinov, *Zh. Priklad Khim.*, 34 (1961) 27.
38 P. Mars, J. J. F. Scholten and P. Zwietering, *Advan. Catal.*, 14 (1963) 35.
39 J. M. Criado, J. Dominguez, F. Gonzalez, G. Munuera and J. M. Trillo, in J. W. Hightower (Ed.), *Proceedings of the Fourth Int. Congr. Catal. Moscow*, Vol. 2, Rice University, Houston, Texas, 1968, p. 676.
40 J. M. Trillo, C. Munuera and J. M. Criado, *Catal. Rev.*, 7 (1972) 51.
41 G. Munuera, *J. Catal.*, 18 (1970) 19.